JOURNAL OF SPACECRAFT AND ROCKETS
Vol. 31, No. 4, July–August 1994

Basic Aerodynamic and Heat Transfer Studies for Spacecraft Boosters in Prelaunch Conditions

L. Scott Miller*
Wichita State University, Wichita, Kansas 67208

A basic experimental investigation was conducted on a simple tandem three-cylinder model to identify potential atmospheric aerodynamic and thermodynamic effects on a typical spacecraft booster configuration during prelaunch conditions. Testing was conducted in a low-speed wind tunnel at a Reynolds number of 100,000. The center and aft cylinders were cooled and heated, respectively, to allow for sustained heat transfer. Flow visualization, anemometry, static pressure, and heat flux measurements were obtained. Results indicate that the model flowfield behavior is very complex and that notable aerodynamic interactions between model elements occur. Most significantly, flow is observed to recirculate about both the cool center and warm aft cylinders. Convective heat transfer maxima were correlated with the identified aerodynamic features. The azimuthal average center and aft cylinder Nusselt-number behavior was found to differ by only about 10%.

Nomenclature

C_p = pressure coefficient, $(P\text{-}P_O)/q$
D = cylinder diameter, m
f = frequency, 1/s
Nu = Nusselt number, $QD/\lambda(T_W\text{-}T_f)$
P = local static pressure, N/m^2
P_O = test section freestream static pressure, N/m^2
Q = heat transfer per unit area, W/m^2
q = dynamic pressure, $0.5\rho V^2$, N/m^2
Re = Reynolds number, VD/ν
St = Strouhal number, fD/V
T_W = surface temperature, °C
T_f = freestream temperature, °C
V = freestream velocity, m/s
λ = thermal conductivity, W/m°K
ν = kinematic viscosity, m^2/s
ρ = flow density, kg/m^3

Introduction

SPACECRAFT typically spend a notable amount of time on the launching pad prior to liftoff and are as a consequence potentially exposed to atmospheric effects. Specifically, aerodynamic and thermodynamic interactions between the spacecraft and the atmospheric flow can be expected to take place. The magnitude of aerodynamic and thermodynamic interactions will depend on many factors, including the specific spacecraft booster geometry or configuration utilized. Many rocket system configurations, currently in use and planned for the future, utilize a large central body/booster and two solid rocket boosters (SRBs).[1-3] Typically, the solid rocket motors are strapped on either side of the large centerbody, which may contain the payload, control systems, rocket engines, and most significantly extremely cold (cryogenic) liquid fuel.

Of particular interest in this discussion are potential atmospheric heat transfer effects on spacecraft boosters of the mentioned configuration during prelaunch conditions. A great deal of both natural and forced convective heat transfer can take place between the cryogenic booster element and the atmosphere. This effect is often evidenced by ice formation on spacecraft exterior surfaces. Unfortunately, this ice can break from the vehicle during launch and impact or damage other parts of the spacecraft.[4] Obviously, ice formation and other heat transfer induced effects can have a notable impact on vehicle operation.

Under some circumstances it appears possible that atmospheric convective heat transfer effects may extend to other, noncryogenic, parts of the vehicle. Specifically, for certain wind directions, the flow moving about the centerbody may be cooled to such a level that it may have the capability to chill other spacecraft elements downstream. Indeed, one of the early causes suggested for the Space Shuttle Challenger disaster included the possible adverse cooling of the right SRB due to convectively cooled atmospheric flow from around the center fuel tank.[5,6] Figure 1 shows a simple diagram illustrating the proposed possible aerodynamic cooling mechanism. First the flow about the cryogenic fuel tank is assumed to be convectively cooled. This chilled flow then interacts with the downwind SRB thus possibly cooling it also. Vectors labeled "Q" indicate the assumed heat transfer directions. Although it is now known that many different factors (most notably the extremely cold weather and the SRB "O-Ring" problem) contributed directly to the Shuttle disaster, potential spacecraft environmental heat transfer problems can still be of concern.

The objective of this work was to examine, experimentally, the aerodynamic and convective heat transfer characteristics of a simple tandem multicylinder model in a transverse flow. The geometry used simulated a spacecraft booster system composed of a large central external tank (ET) flanked by two SRB elements. The center and downwind cylinders were cooled and heated, respectively, to induce heat transfer. Tests were con-

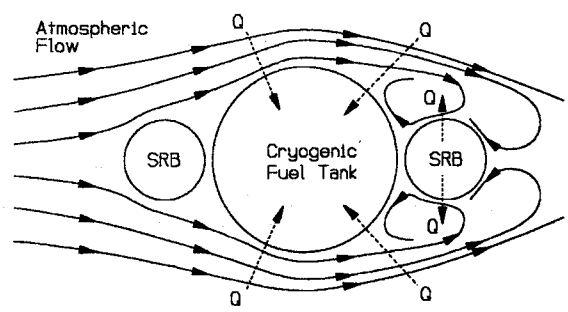

Fig. 1 A possible atmospheric cooling mechanism for a downstream solid rocket booster (SRB).

Received July 4, 1992; revision received Oct. 8, 1992; accepted for publication Oct. 16, 1992.

*Assistant Professor, Department of Aerospace Engineering, Member AIAA.

ducted in a low-speed wind tunnel utilizing flow visualization, laser Doppler anemometry (LDA), constant temperature anemometry (CTA), surface static pressure, and heat flux measurement techniques. Data from the investigation can potentially be used to identify aerodynamic and thermodynamic interactions between a spacecraft booster (of the specified configuration) and the atmosphere during prelaunch conditions.

Experimental Facilities, Apparatus, and Methods

A detailed description of the facility, instrumentation, and methods utilized to identify the aerodynamic and thermodynamic character of the three-cylinder model is provided in the following.

Wind Tunnel

The experimental investigation was conducted in the Texas A&M University 0.45 × 0.45-m cross section induction-type low-speed wind tunnel, fitted with a 25:1 contraction ratio inlet and eight layers of turbulence suppressing screens. For the investigation, the test section turbulence intensity was less than 0.5% at 27.0 m/s. This flow operating condition corresponds to a Reynolds number of 100,000 based on the test model center cylinder diameter. Test-section (freestream) airspeed and temperature were recorded upstream and below the model, using a Pitot-static probe and a thermistor-type temperature sensor. Test-section speed was maintained within about 1.0 m/s. Freestream temperature varied on a daily basis but averaged about 18.0 °C over the duration of testing.

Model Geometry

A simple diagram of the model utilized in the investigation is provided in Fig. 2. As can be seen, the model is composed of three cylinders of two different diameters oriented in tandem. The center and two flanking cylinders are 5.72 cm and 2.45 cm in diameter, respectively. The gap or spacing between cylinders is 0.26 cm. Once positioned in the wind tunnel, the model extended horizontally from wall-to-wall and thus constituted a two-dimensional installation. This horizontal model orientation was necessary to facilitate LDA measurements.

Typical spacecraft booster configurations operate at a full-scale Reynolds number of approximately one million while on the launch pad. As was mentioned, the current investigation was performed at a Reynolds number of 100,000. When model size or tunnel limitations prevent operation at desired (typically higher) Reynolds number conditions, it is common practice to utilize boundary-layer trips. These trips are intended to "simulate" higher Reynolds-number conditions by promoting earlier boundary-layer transition. Unfortunately, boundary-layer trips could not be used on the current model due to the way the model was constructed. As will be discussed in greater detail shortly, each model cylinder only had one set of pressure, temperature, and heat flux transducers. To identify azimuthal pressure, temperature, and heat flux levels the cylinders were simply rotated. This measurement procedure unfortunately prevents the use of boundary-layer trips on the model but has the advantage of minimizing model construction expenses and complexity.

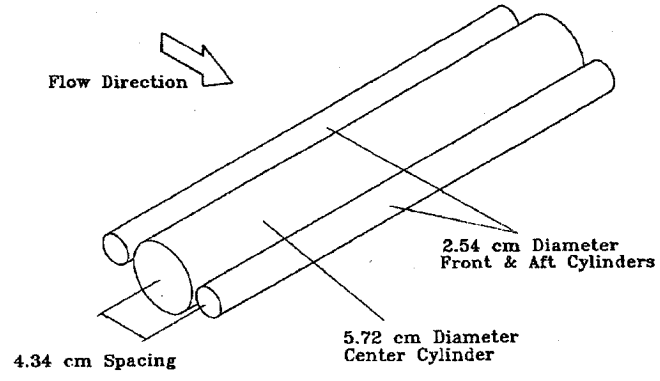

Fig. 2 Diagram of the three-cylinder test model.

Temperature Control

As was mentioned previously, the center and aft model cylinders were respectively cooled and heated to promote sustained heat transfer with the surrounding flow during tests. A pump continually cycled 1.0 °C water from a large insulated tank containing an ice-water mixture through the center cylinder. Warm 35.0 °C water was continuously cycled through the aft cylinder. Baffles, installed inside each cylinder, insured uniform water mixing and interaction with the cylinder interiors. The circumferential temperature distribution over the cylinder surface, at the thermocouple spanwise location, was observed to be nearly uniform (with less than 2 °C variation) with the wind on. Surface temperature measurements over the span of the model were not obtained due to instrumentation limitations.

Model Static Pressures

A single pressure tap was installed on the center and one of the smaller model elements in order to allow for surface pressure measurements. Azimuthal static pressure data was obtained by simply rotating (with approximately one-degree accuracy) each model element, and thus the pressure tap, about the cylinder axis during tests. A tap was installed in only one small cylinder since the cylinder was interchangeable between the front and aft locations. This feature minimized model shop work for tap and other sensor installation. The 0.051-cm-diam pressure taps were installed 20.3 cm from the cylinder end, with care to assure that the opening was flush and smooth with the surface.

Each model tap was connected by tygon tubing to a Validyne Corporation pressure transducer and signal conditioning unit. The electrical output from each transducer represented the difference between the measured pressure and the tunnel test-section static pressure, as recorded by the static port on the Pitot-static probe. A third transducer continuously measured test-section dynamic pressure. To assure consistent and reliable measurements each transducer was calibrated daily. This measurement system allows for the resolution of pressure coefficient changes of ± 0.0015.

Model Heat Flux and Temperature Behavior

Heat flux gauges, with integral thermocouple temperature sensors, were installed near the static pressure ports on two of the model cylinders. Each sensor combination, made by RdF Corporation, was mounted approximately 0.03 cm below the surface and 15.0 cm from the cylinder end. The 0.25 × 0.25 cm heat flux gauge was covered by a thin layer of silver epoxy and the adjoining thermocouple, located 0.51 cm away, was covered by a thin layer of silicon adhesive. Silver epoxy, which is an excellent heat conductor, was utilized to minimize effects on heat transfer from or into the cylinder while simultaneously facilitating gauge mounting. Silicon, which is a poor heat conductor, was utilized to assure that the thermocouple sensor measured cylinder surface temperatures and not the adjoining flow temperature. Both the silver epoxy and silicon coverings were carefully applied and shaped to maintain cylinder surface smoothness and contour. As with the static pressure taps, the azimuthal heat flux behavior could be determined by rotating each model cylinder. Temperature and heat flux measurements were used to calculate local Nusselt-number values, based on gauge calibration data supplied by the sensor manufacturer.

Oscilloscope observations indicated that a high-frequency noise signal, perhaps from the tunnel motor control unit, was present in the heat flux thermocouple gauge output signals. In light of this problem, the signals were low-pass filtered prior to data acquisition. The impact of this problem was minimal since only average heat flux information was desired. An amplifier with a gain of 2000 was used to boost the heat flux gauge output level to a value better suited for recording. A full calibra-

tion was performed, using a microvolt power supply standard, prior to each run to accurately identify amplifier and filter gain and zero offset values. The heat flux measurement system allows model Nusselt-number behavior identification within a level of approximately ± 5.0.

Laser Doppler Anemometry

A one-component TSI (Thermal Systems, Inc.) backscatter LDA system, fitted with a frequency shift module, was utilized to make two-component average velocity measurements in a plane about the model. Although this is a one-component system, the second velocity component was obtained by mechanically rotating the measuring volume 90 deg. The system used a 35-mW Helium-Neon (HeNe) laser and a 1.0-m focal length (155 mm diam) objective lens which produced a measuring volume of 0.133 mm diam. Use of a frequency shifter allowed for reversed flow identification. Six thousand samples were obtained for each average two-component velocity measurement. A TSI counter processor gathered, conditioned, and transmitted the data directly to the computer data-acquisition system. At each measurement location, the required number of samples were obtained typically over about a 10–30 s time period.

Seeds, generated by atomizing a sugar-water mixture, were injected into the wind-tunnel inlet and entrained into the test-section area about the model. During transit to the test-section area, it is assumed that most of the water evaporated leaving a large number of approximately 1.0-μm-diam sugar particles. Light scattered by these particles was used by the LDA system to calculate the flow velocity.

The entire LDA system was mounted on a traversing rig which moved to provide measurements in a vertical plane, perpendicular to the model, at the half-span location. This traversing mechanism provided 0.02-mm measuring volume positioning accuracy in three directions. The flow speed and direction was measured during tests along 12 lines or stations around the model. Vertical measurement intervals ranging from 0.12–0.51 cm were used on each line, depending on the flow behavior, desired detail, and station location.

Constant Temperature Anemometry

A CTA system and spectrum analyzer were utilized to identify wake dynamic characteristics. The single sensor hot-film probe could be positioned at a number of different locations within the model wake. Velocity data from this sensor was input to a fast Fourier transform-based spectrum analyzer unit to identify possible model periodic wake velocity variations. All measurement results presented, in the following, were taken at a position 0.63 cm below the tunnel centerline and 10.79 cm downstream of the model. At this location, significant peaks in the wake velocity spectrum were observed. (This result will be discussed in greater detail later.)

Flow Visualization

The kerosene/tempera flow visualization method was utilized to identify general model surface flow features, including separation and reattachment areas. Prior to testing, a liquid kerosene and tempera powdered paint mixture was applied to the model. During wind-tunnel operation the solution moved, under the influence of shear forces, to establish patterns indicating significant on and off surface flow features. After a necessary time period the kerosene evaporated leaving a tempera paint residue on the model, thus preserving flow patterns for later viewing. The kerosene evaporation rate was controlled by adding small amounts of general-purpose oil to the solution. Flow features unique to the exact test conditions, and not tunnel startup for example, were thus recorded.

A smoke cloud, produced by the vaporization of a glycol solution, was injected into the upstream flow and illuminated using a 5.0 W argon-ion laser. The light beam from the laser was aimed through a cylindrical lens which produced a sheet of light positioned perpendicular to the model axis at the half-span location. A thin plane or cross section of the smoke flow surrounding the model was thus illuminated, showing the general behavior of the model flowfield in a two-dimensional plane.

Data Acquisition

Appropriately conditioned signals from the LDA, pressure, temperature, and heat flux instrumentation were sent to a personal computer (PC) based data-acquisition system. Measurements from the various sensors (except the LDA) were collected using a 16-channel, 12-bit, analog-to-digital (A/D) converter which was software-controlled by the PC. The A/D board acquired 1000 samples, sequentially, from each sensor at a rate of 300 samples/s. LDA data was transferred directly to the PC through a TSI communications board. Data received from the A/D board were recorded in raw form on both the hard and floppy disk drives. Limited real-time calculation and display of average quantities were utilized during tests for monitoring purposes. More detailed raw data analysis was performed following the tests.

Results

Complex model flowfield and convective heat transfer features were identified in detail.[7] The following sections present and discuss in relative detail flow visualization, LDA, CTA, static pressure, and heat transfer results. All testing was performed for a tandem cylinder configuration. Unfortunately, due to time constraints, no other flow directions were examined.

With respect to the following discussions, keep in mind that only upper surface results are discussed. Features on the bottom are assumed identical since the model is symmetrical. The locations of significant aerodynamic or thermodynamic peculiarities on each cylinder are referenced using angular coordinates. The 0- and 90-deg locations correspond, respectively, to the upstream horizontal and top cylinder positions.

Flow Visualization Results

Flow visualization experiments, utilizing kerosene/tempera and smoke methods, demonstrated that the model aerodynamic features are very complex. All visualization work was performed at 27.0 m/s and with the model at freestream temperature. A photograph of the model flow features is shown in Fig. 3 and schematic summary of the significant results is shown in Fig. 4. Note that the freestream direction is right to left in both of these figures.

Starting with the front cylinder, a stagnation line extending along the entire leading edge is observed at the 0-deg location.

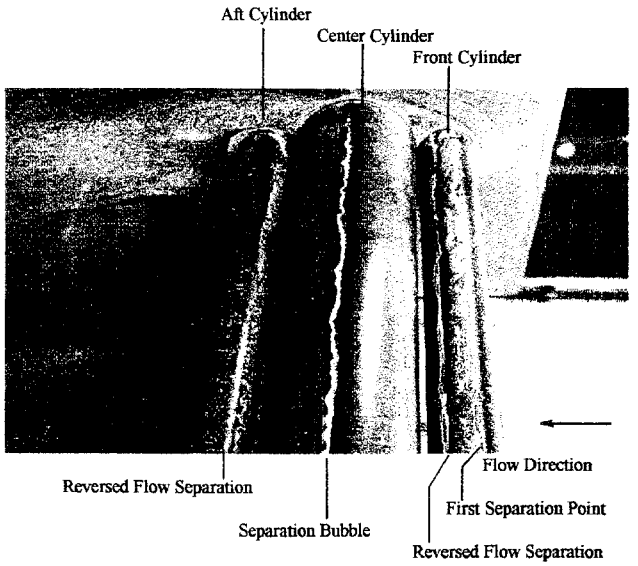

Fig. 3 Flow visualization photograph of the three-cylinder model in the wind tunnel. (Flow direction is right to left.)

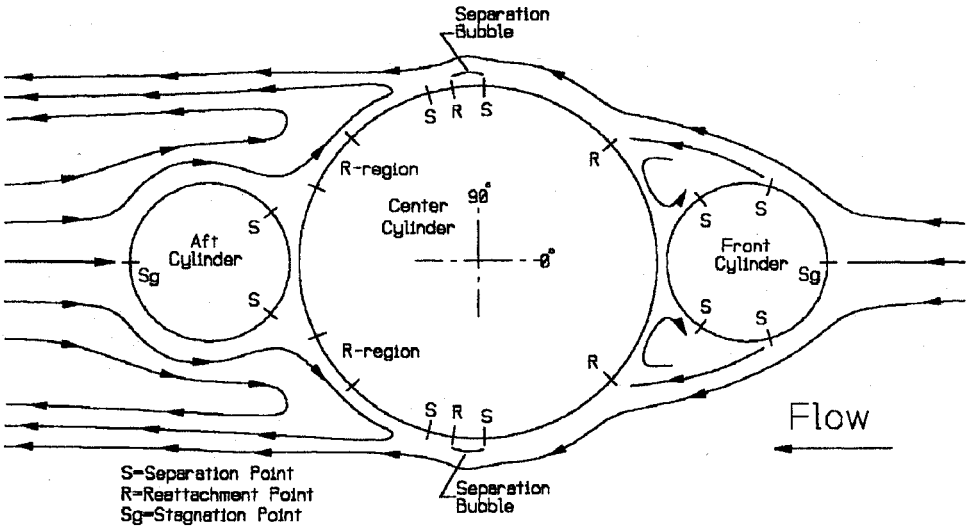

Fig. 4 Flow visualization results summary. (Flow direction is right to left.)

The flow moves upward over the cylinder until approximately the 75-deg location, where flow separation occurs. This separated flow continues moving in the downstream direction toward the center cylinder. A region of nondistinct low velocity flow, which hardly disturbs the surface visualization mixture, extends over the next 50 deg of the front cylinder. At the 125 deg location, another flow separation line is observed. This separation line is, however, due to a reversed flow leaving the area between the front and center cylinders, where a standing recirculating flow pattern is observed.

Figures 3 and 4 also identify the notable flow features around the center cylinder. A "stagnation like" reattachment line is observed at the 42-deg location, as a result of the impingement of the separated flow from the front cylinder. Above this line the flow moves upwards, and below this line the flow moves downward. The downward flow combines with the previously noted recirculating flow present in the front and center cylinder junction region. The upward moving flow separates at the 88-deg location and then reattaches approximately 10 deg later. Significantly, the flow between the 88- and 98-deg locations moves slowly in the upstream direction. After reattachment at the 98-deg location, the flow again separates this time at the 106-deg position. Flow behavior such as this (separation, reattachment, and then separation again) is consistent with the presence of a laminar separation bubble.[8]

The existence of a laminar separation bubble, on the current three-cylinder model, suggests a more "critical" flow behavior than the test Reynolds number might imply. Laminar separation bubbles are commonly observed on simple cylinders operating in a Reynolds-number range around 450,000. Laminar boundary-layer separation, at about 75 deg without bubble formation, would normally be expected for a simple cylinder operating at a Reynolds number of 100,000. The presence and effect of the front cylinder apparently promotes the occurrence of a laminar separation bubble as opposed to simple laminar separation.

Over the aft side of the center cylinder, from 135 to 155 deg, a "stagnation region" is observed. Interestingly, a wide region of impinging flow, instead of a distinct stagnation line, is noted. As will be discussed later, the flow behavior downstream of the center cylinder was very unsteady. This flow unsteadiness may prevent the formation of a distinct stagnation line. The flow moves downward and upward, respectively, below and above the stagnation region. A small pocket of standing recirculating flow exists in the junction area between the aft and center cylinders. Above the stagnation region, the flow continues moving upward eventually turning downstream.

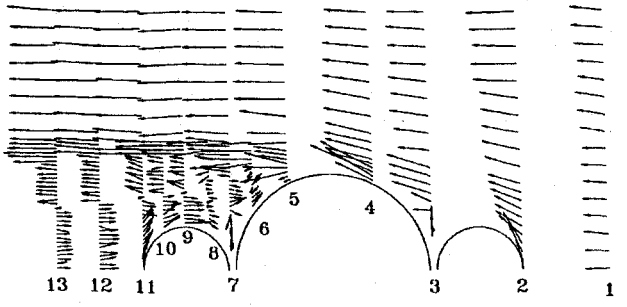

Fig. 5 Average two-component LDA velocity measurements. (Flow direction is right to left.)

Visualization results, around the aft cylinder, indicate that this element is almost completely immersed in reversed flow. Flow separation is observed to occur at the 40-deg location, however. Significantly, this separated reversed flow moves toward the previously noted "stagnation region" present on the aft side of the center cylinder. Unfortunately, the exact behavior of the wake flow downstream of the model was difficult to identify from the visualization investigations. Further information related to the wake character will be offered in the following sections.

Laser Doppler Anemometer Results

LDA measurements and the resulting two-component average velocity data obtained for the model at freestream temperatures are shown in Fig. 5. As was the case for flow visualization results, please note that the freestream flow is from right to left. Also recall that the freestream velocity was 27.0 m/s. The right most (station 1) velocity vector lengths thus represent approximately 27 m/s airspeed. The magnitude of other vectors can be compared according to this datum.

Great care should be exercised to note that these results represent the average flowfield velocity behavior over an extended period of time. Instantaneous flow velocity measurement will likely differ significantly. Indeed, as the velocity spectrum data will show, the wake flowfield was quite unsteady.

Velocity measurements along station 3, shown in Fig. 5, confirm that there is downward flow into the area between the center and front cylinders. Interestingly, a single velocity vector can be seen to point, approximately, toward the noted center

cylinder flow reattachment location. At the lowest measured position along station 5, a single low velocity vector can be seen to point in the upstream direction where flow visualization results indicated flow separation occurred. Data along station 7 suggest that flow stagnation, at the previously noted position, on the center cylinder aft side is indeed occurring. Measurements along stations 8–13 confirm that the aft cylinder is enclosed by reversed flow.

As can also be seen in Fig. 5, two approximately horizontal shear lines exist within the model wake region. The inner shear line divides low-speed oppositely moving (reversed and downstream) flows. The upper shear line divides downstream moving high- and low-speed flows. It is postulated that the low-speed flow, above the inner shear line, extends downstream where it turns inward and reverses to move over the aft cylinder. A nearly closed, recirculating flow over the aft cylinder and part of the center cylinder is thus assumed to exist. Unfortunately, direct verification of this hypothesis was not possible. LDA measurements aft of station 13 were not obtained due to the extremely unsteady nature of the flow. Flow turbulence intensity levels, identified from CTA measurements, ranged from 15 to 30%.

Constant Temperature Anemometry Results

As was mentioned in the discussion of the visualization and LDA results, the wake flowfield behavior was very unsteady. Identification of wake velocity fluctuation (frequency) spectrum was used to verify the presence of significant flow features, such as Karman-type vortex streets. Hot-film sensor measurements indicate that a notable amount of velocity fluctuation energy is present over a frequency range from 0 to 250 Hz, as shown in Fig. 6. A peak, of notable amplitude, occurs at a frequency of 135 Hz. This frequency corresponds to a Strouhal number of 0.275, based on the center cylinder diameter. As a point of reference, the Strouhal number for a single cylinder of the same diameter is 0.21. This result suggests that a periodic vortex type wake may be developing behind the model.

Static Pressure Measurement Results

Figures 7–9 identify the azimuthal static pressure coefficient variations about all three model elements. For comparison purposes, the static pressure variation of a simple cylinder operating at a Reynolds number of 100,000 is shown on each of the results plots.[8]

Figure 7 shows that the model front cylinder pressure coefficient distribution. The extent of constant pressure confirms the existence of flow separation identified from flow visualization investigations. As a result of a comparison with the simple cylinder results, the presence of the downstream (center and aft) cylinders is such as to reduce the flow velocity about the front cylinder.

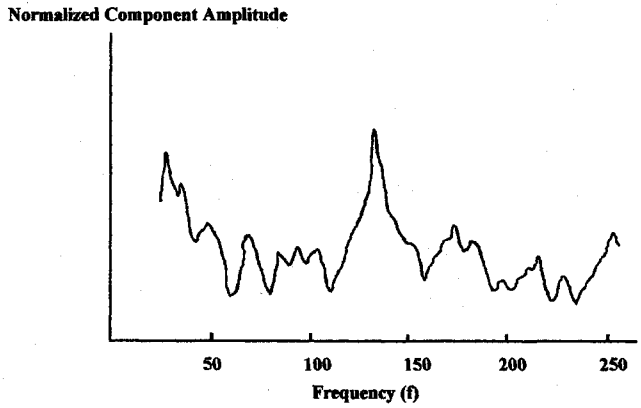

Fig. 6 Wake velocity spectrum from CTA measurements.

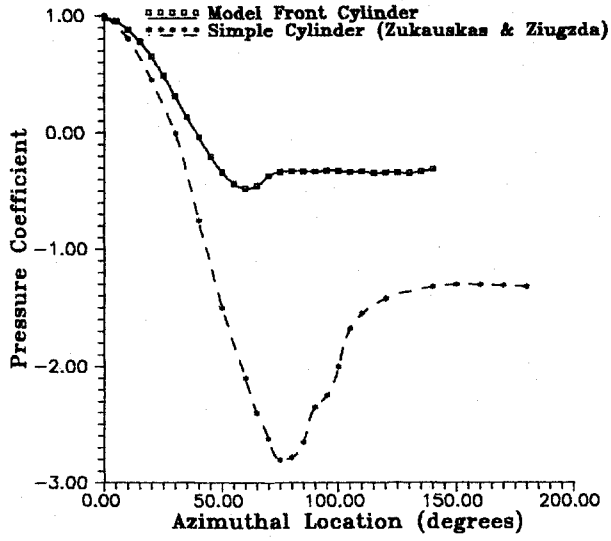

Fig. 7 Front cylinder surface static pressure distribution.

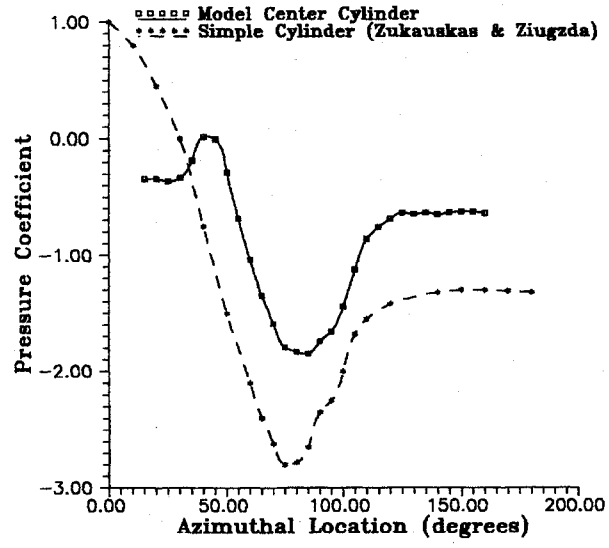

Fig. 8 Center cylinder surface pressure distribution.

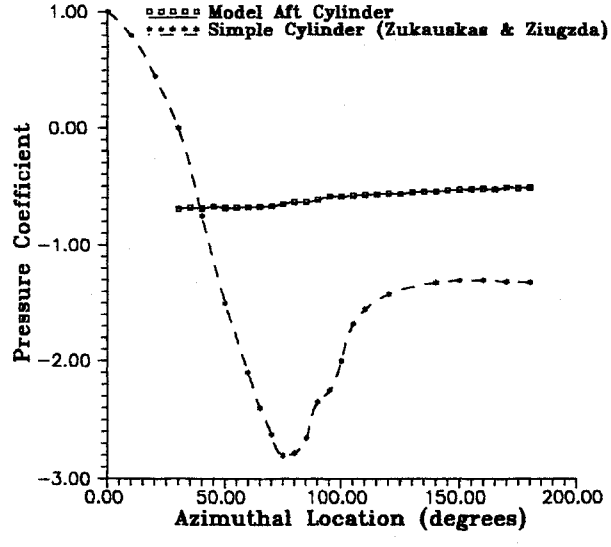

Fig. 9 Aft cylinder surface static pressure distribution.

Center cylinder results, shown in Fig. 8, indicate a high-pressure level at the 40-deg location where flow visualization and LDA results indicated the separated flow from the front cylinder reattached. The occurrence of a separation bubble is noted by a small deviation in the pressure distribution between the 85- and 95-deg locations. When compared to a simple cylinder, the presence of the front (and perhaps the aft) cylinder appears to moderate the magnitude of the flow velocity about the center cylinder.

Figure 9 shows that pressure coefficients about the aft cylinder are nearly constant. The pressure level is of the same magnitude as measured on the aft side of the center cylinder (see Fig. 8). In light of this observation, the flowfield behavior of the aft cylinder appears to be dominated by that of the center cylinder.

Heat Transfer Results

Figures 10 and 11 show the Nusselt-number variation about the model center and aft cylinders. Because of time limitations, front cylinder heat transfer data was not obtained. For comparison purposes, the Nusselt-number variation of a simple cylinder operating at a Reynolds number of 100,000 is shown on each of the plots.[9]

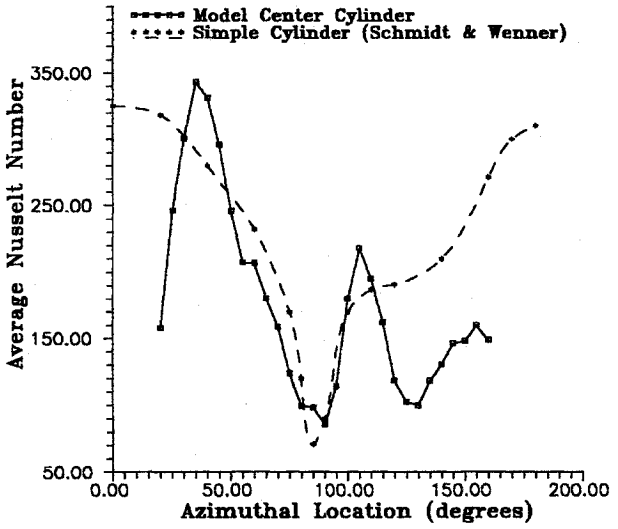

Fig. 10 Center cylinder azimuthal convective heat transfer behavior.

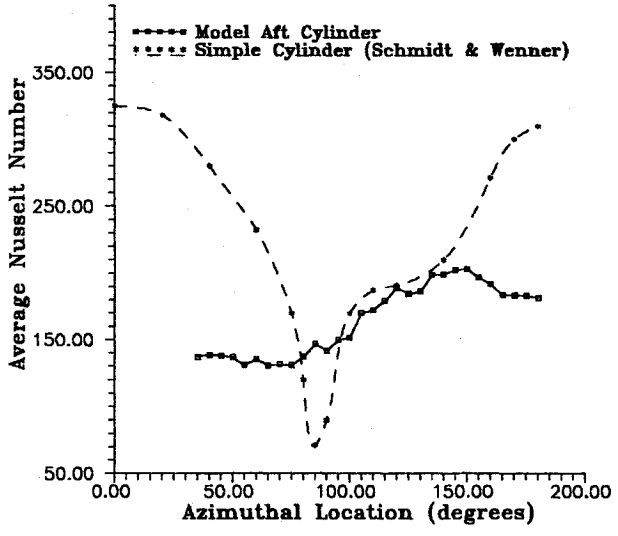

Fig. 11 Aft cylinder azimuthal convective heat transfer behavior.

As can be seen in Fig. 10, two local Nusselt-number maxima exist on the center cylinder. These peaks indicate relatively strong levels of convective heat transfer are taking place between the surrounding flow and the center cylinder. The largest local Nusselt-number value occurs at the 35-deg point, or slightly forward of the front cylinder separated flow reattachment location. The second heat transfer maxima occurs at the 105-deg location. This is the location where flow separation from the center cylinder occurred. Minimum heat transfer levels occur at the 90- and 125-deg locations. As can be seen in Fig. 11, the aft cylinder shows a much smoother Nusselt-number variation than the center cylinder. The average Nusselt-number magnitude for the center cylinder was 176 and that for the aft cylinder was 158. This result represents about a 10% difference.

When compared to a simple cylinder, the effect of a smaller upstream cylinder appears to be azimuthally dependent, both decreasing and increasing the local heat transfer behavior of the center cylinder (see Fig. 10). Low Nusselt numbers are observed in the junction area next to the front cylinder and high Nusselt numbers are produced as a result of the front cylinder separated flow reattachment. The center model element has comparable or lower levels of heat transfer taking place with the surrounding flow at other azimuthal locations. The presence of the aft, and possibly the front, cylinder is such as to reduce the local Nusselt-number magnitude on the back side of the center cylinder. When compared to a simple cylinder (see Fig. 11), the aft model element has a notably lower overall heat transfer level with the surrounding flow. The presence of upstream model elements apparently diminishes the magnitude of the Nusselt numbers.

Conclusions

An experimental investigation was conducted to identify potential atmospheric aerodynamic and thermodynamic effects on spacecraft boosters during prelaunch conditions. A simple tandem three-cylinder model, resembling some booster configurations, was tested in a low-speed wind tunnel at a Reynolds number of 100,000. Flow visualization, static pressure, anemometry, and convective heat transfer data were obtained and presented. The following conclusions are offered based on the investigation results.

1) The model flowfield characteristics are very complex. Flow visualization and static pressure measurements identified significant flow features and separation and reattachment points on each model element. Notably, separated flow from the front cylinder reattaches on the front side of the center cylinder. The front cylinder appears to induce the presence of a laminar separation bubble and more "critical" Reynolds-number conditions on the center cylinder. The aft cylinder is fully immersed in a reversed and recirculating flow which interacts notably with the aft side of the center cylinder.

2) LDA data confirms that notable flow recirculation between the center and aft cylinders takes place. These results correlate well with flow visualization and static pressure measurements and suggest a mechanism for possible adverse convective cooling of a downwind booster element.

3) CTA measurements suggest that a periodic vortex wake, with a Strouhal number of 0.275, forms downstream of the model (at this Reynolds number).

4) A notable amount of convective heat transfer takes place between the flow and the chilled center cylinder. Local Nusselt-number maxima correspond with identified aerodynamic features. The average aft cylinder convective heat transfer (cooling) level is similar in magnitude to the average (heating) observed for the center cylinder.

References

[1] "Martin Marietta Poised to Adapt External tank for NLS Core Vehicles," *Aviation Week and Space Technology*, Aug. 26, 1991, pp. 58–60.

[2]Hanley, A., "Titan IV: Latest in a Family of Giants," *Aerospace America*, July 1991, pp. 34–38.
[3]DeMeis, R., "New Life for Heavy Lift," *Aerospace America*, March 1992, pp. 32–35.
[4]Porteiro, J. L. F., Norton, D. J., and Pollock, T. C., "Space Shuttle Ice Suppression System Validation," Texas Engineering Experiment Station, Rept. TEES-TR-4587-82-01, Texas A&M Univ., College Station, TX 1982.
[5]"Wind Tunnel Data Indicated Potential for Frozen Seals," *Aviation Week and Space Technology*, Feb. 24, 1986, pp. 22–25.
[6]Porteiro, J. L. F., "Shuttle Wind Tunnel Test Data Clarified," *Aviation Week and Space Technology*, March 31, 1986, pp. 147, 148.
[7]Miller, L. S.,"Basic Flow Field and Heat Transfer Studies About Three Cylinders of Different Diameter in Transverse Flow," Ph.D. Dissertation, Texas A&M Univ., College Station, TX, Aug. 1988.
[8]Zukauskas, A., and Ziugzda, J., "Fluid Dynamics on a Cylinder," *Heat Transfer of a Cylinder in Crossflow*, Hemisphere, New York, 1985, p. 154.
[9]Schmidt, E., and Wenner, K., "Heat Transfer Over the Circumference of a Heated Cylinder in Transverse Flow," NACA TM 1050, 1943.

E. Vincent Zoby
Associate Editor